Electronic Supplementary Material (ESI) for CrystEngComm.

Control of interpenetration of Copper-based MOFs on supported surfaces by electrochemical synthesis

Sumit Sachdeva,[a,b] Alexey Pustovarenko,[b] Ernst Sudhölter,[a] Freek Kapteijn,[b] Louis C.P.M de Smet[a] and Jorge Gascon[b,*]

[a] Organic Materials and Interfaces, Department of Chemical Engineering, Delft University of Technology, Delft, The Netherlands.
[b] Catalysis Engineering, Department of Chemical Engineering, Delft University of Technology, Delft, The Netherlands.

Supporting information

1. Experimental Details

All chemicals were purchased from Sigma Aldrich as used as received. The electrode used were made from 99.9% pure copper. The electrodes were inserted between 2 PTFE plates, which only allowed a small square opening (6.26 mm × 6.26 mm) to be in contact with the synthesis solution. The potentiostat used was an AUTOLAB PGSTAT302N.

Scanning Electron Microscopy (SEM) images were obtained with a JEOL JSM 6010LA setup. N_2 and CO_2 sorption analysis were carried out in a Micromeritics instrument Tristar II. The samples were pre-treated before measurement by outgassing under vacuum at a temperature of 393 K for 16 hrs.

The powder X-ray diffraction measurements were performed on a Bruker D8-Advance diffractometer operated in Bragg-Brentano geometry, equipped with a Co-Kα source (λ = 1.78897 Å). The diffraction data for MOFs found in bulk were collected over an angle range from 5° to 62° and for MOFs samples obtained on the electrode surface from 2° to 80° with a step width of 0.02° and scan speed of 0.2°/s.

2. Electrochemical synthesis of Copper MOFs

a. Synthesis of MOFs as bulk powder

200 mg of linker (H_3BTC or H_3TATB) and 25 mg of electrolyte (MTBS) were dissolved in 8 mL of 96% ethanol. The solution was mixed in a home-built, Teflon electrochemical cell (~10 mL, see literature for details of larger version of this cell[1]) at either room temperature or 70 °C for high-temperature synthesis with two copper electrodes spaced 2.4 mm apart. Constant current of 1 mA was applied for 10 h to obtain the material in solution. The material was then filtered and washed with ethanol overnight at 75 °C. The material was then filtered again and dried at 100 °C for 2 h.

b. Synthesis of MOFs as surface supported film

100 mg of linker (H_3BTC or H_3TATB) and 25 mg of electrolyte (MTBS) were dissolved in 8 mL of 96% ethanol. The solution was mixed in the electrochemical cell at room temperature with two electrodes, copper mesh as anode and copper electrode as cathode, which were spaced 2.4 mm apart. Cyclic pulses of 2 mA/5 s and 0 mA /5 s (or 1 mA/5s and 0 mA/5s) were applied for 12 cycles (60 s of current). The meshes were washed with ethanol at room temperature overnight and dried at 100 °C for 2 h

c. Optimization procedure for surface growth

3.15 g of H_3BTC and different concentrations of MTBS (155-623 mg, i.e. 0.5-2 mmol) were dissolved in 100 mL of 96% ethanol. The solution was mixed in the electrochemical cell at room temperature with two copper electrodes spaced 3 cm apart with a circular opening of 25 mm in contact with solution (area 4.9 cm^2) . Cyclic pulses of 50 mA/5 s and 0 mA/5 s were applied to keep the current density constant with other experiments. Different pulse cycles were applied to obtain the crack-free uniform layer. The meshes were washed with ethanol overnight and dried at 100 °C for 2 h.

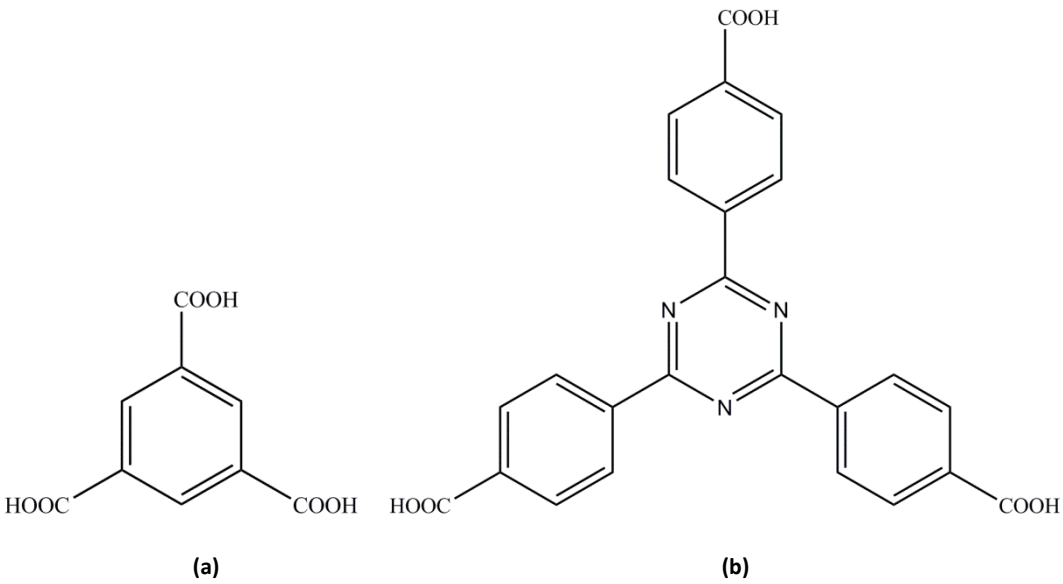

Figure S1. Molecular structures of the two linkers used in the study:H_3BTC (a) and H_3TATB (b).

3. Powder X-ray diffraction, refinement and structural details for MOFs obtained in bulk and surface-supported.

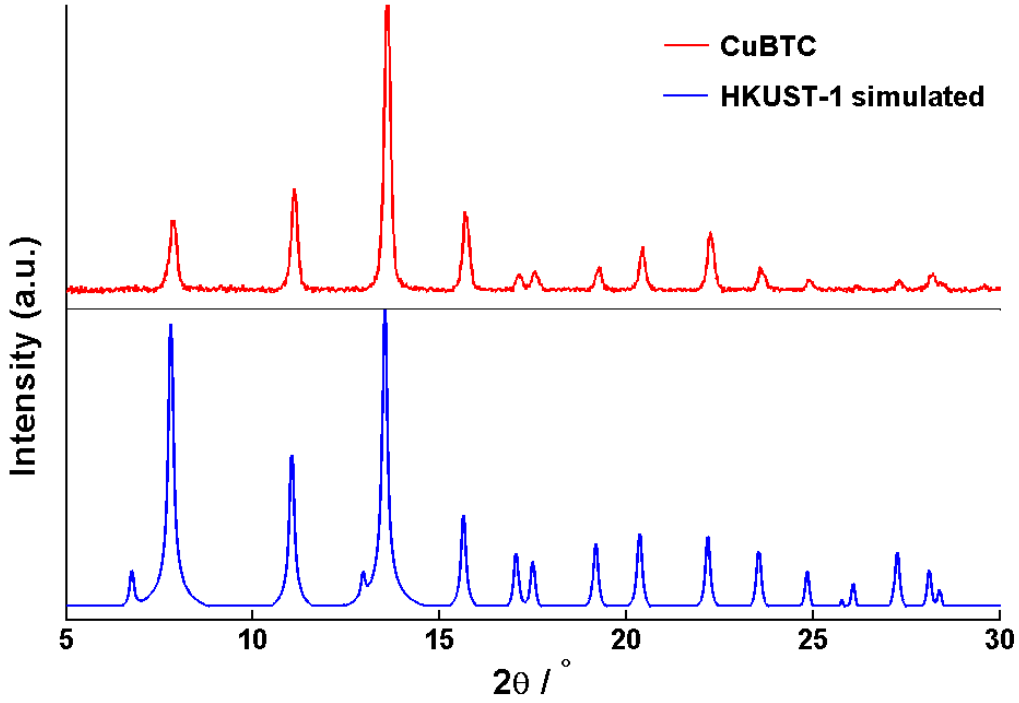

Figure S2. Comparison of XRD patterns of CuBTC obtained in bulk (experimental) and HKUST-1 (simulated).

Rietveld refinement of CuTATB obtained in bulk has been performed with EXPO2014 [2], by which zero offset, scale factor, eight background terms and profile parameters as a PearsonVII function were refined.

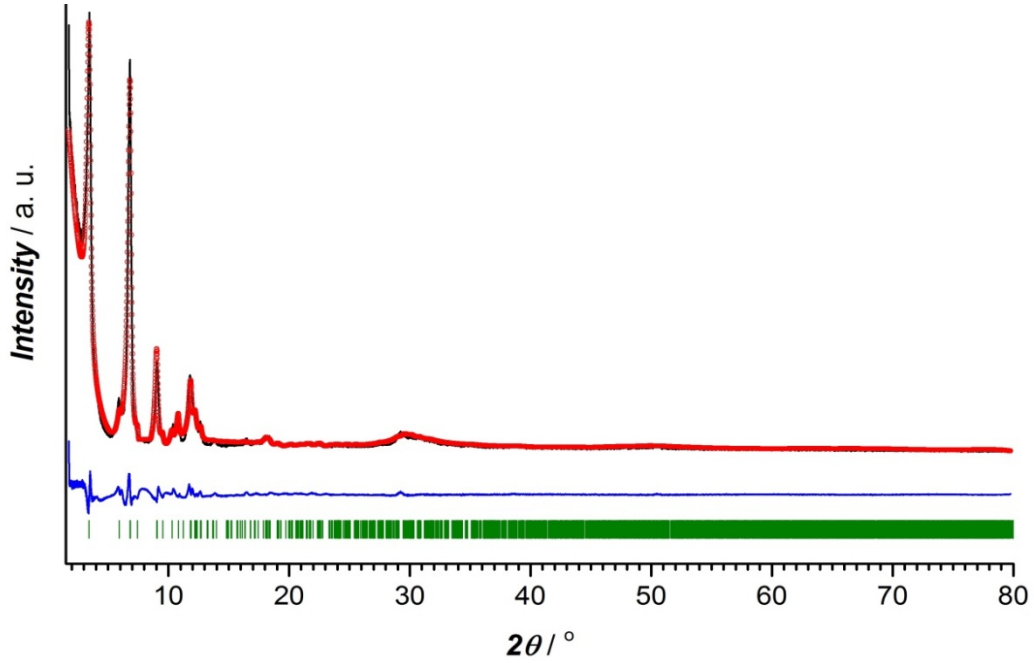

Figure S3. Rietveld refinement plot for CuTATB MOF obtained in bulk. The experimental data are presented as black solid line, the calculated data by red circles and difference as blue solid line. The Bragg positions of the peaks are represented as green sticks.

Table S1. Unit cell parameters for CuTATB (obtained in bulk) determined by Rietveld refinement of experimental XRD pattern and compared with CuBTB [3]

Compound	**CuTATB**	**CuBTB**
Formula	$C_{100}\ H_{57}\ Cu_4\ N_{12}\ O_{28}$	$C_{456}\ H_{308}\ Cu_{16}\ O_{142}$
FW / g·mol^{-1}	2128.78	9075.84
Crystal system	Orthorhombic	Orthorhombic
Space group	*Pbcm*	*Pbcm*
a / Å	29.9203(20)	28.0524(17)
b / Å	17.3963(9)	14.8658(9)
c / Å	34.5860(17)	28.7818(18)
α / °	90	90
V / Å^3	18002.2(10)	12002.6(13)
Z	4	1
R_1,[i] wR_2[ii]	9.290, 12.917	–

[i] $R_P = \Sigma_i|y_{i,0} - y_{i,c}|/\Sigma_i|y_{i,0}|$; [ii] $R_{wp} = \left[\Sigma_i w_i(y_{i,o} - y_{i,c})^2 / \Sigma_i w_i(y_{i,o})^2\right]^{1/2}$

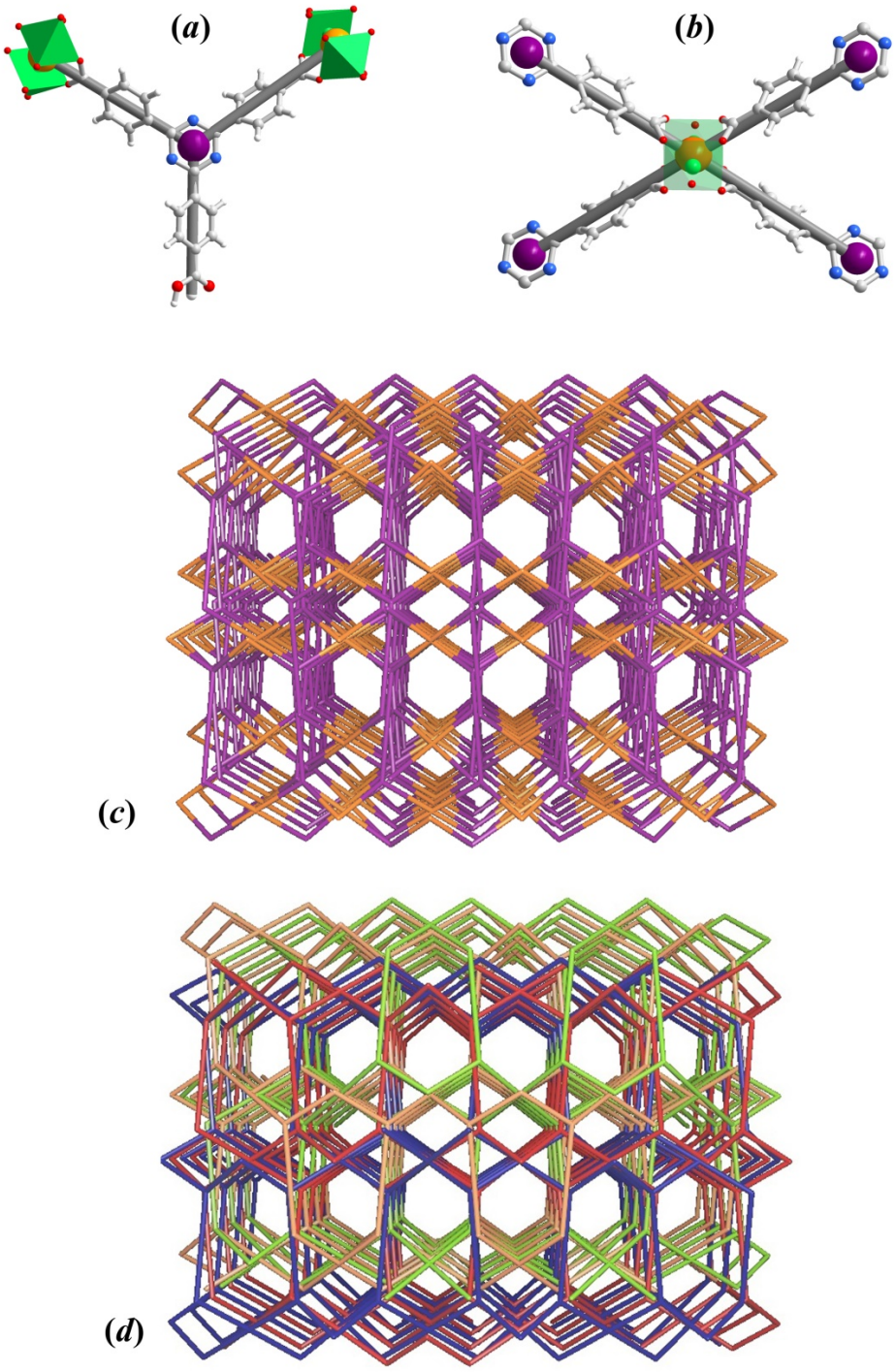

Figure S4. Simplification of CuTATB structural units: (a) TATB tripod linker represented as a 3-connected node; (b) paddlewheel cupper unit represented as a 4-connected node. (c) Topological view of CuTATB highly interpenetrated net where 3-c nodes of TATB are drawn as violet centres and 4-c nodes of dimeric copper unit as orange centres. (d) The four-component interpenetration in CuTATB polymeric network where each independent polymeric frame is binodal 3,4-connected of sur topological type (each independent net is drawn with different colour).

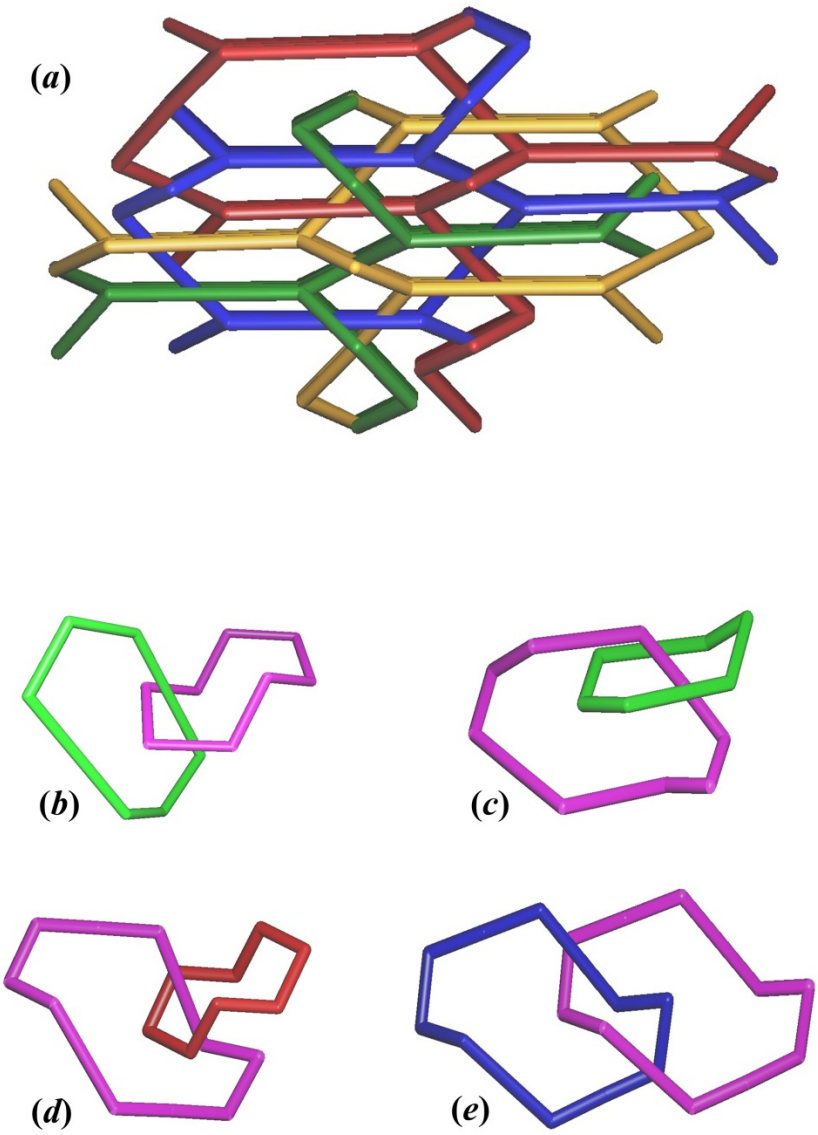

Figure S5. (a) Four interpenetrated nets forming array of CuTATB which show four different links (knots) of Hopf type between closed circles: (b) 6-membered (green) and 8-membered (magenta); (c) 8-membered (green) and 8-membered (magenta); (d) 8-membered (red) and 10-membered (magenta); (e) 10-membered (blue) and 10-membered (magenta)

Topological analyses of CuTATB structures have been performed using ToposPro software package [4]. All the interpenetration nets have the topology of ***sur***-type net and the interpenetration type belongs to a rare class IIIa [5]. As shown in Fig. S5, the interpenetration of four equivalent ***sur***-nets realized by four kinds of interwoven rings (Hopf links): six- and eight-membered rings (b); eight- and eight-membered rings (c); ten- and eight-membered rings (d); ten- and ten-membered rings (e).

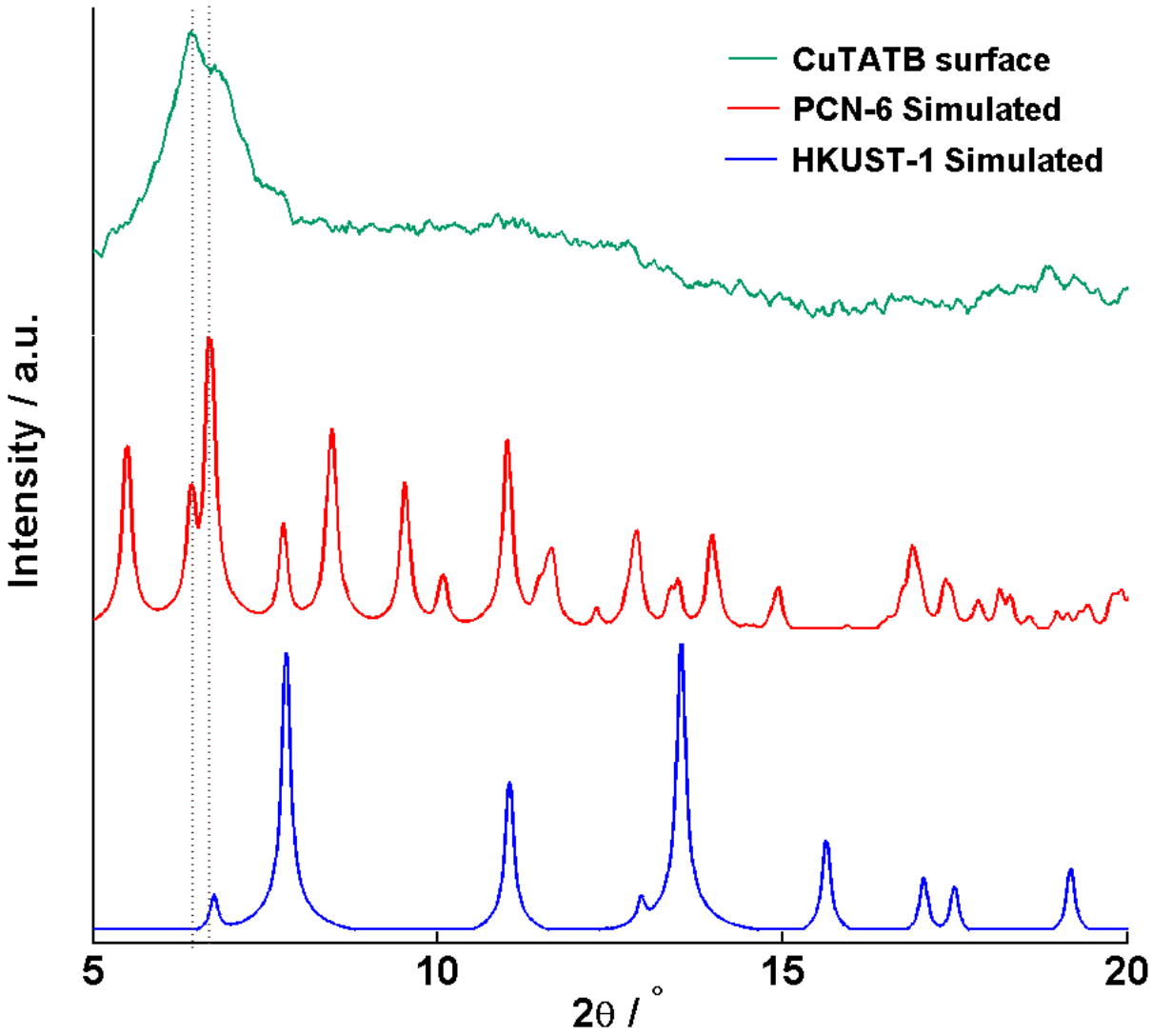

Figure S6. Comparison of the pattern of CuTATB scratched from the electrode surface (green) and simulated patterns of PCN-6 structure (red) and HKUST-1 (blue). The dashed lines indicate the most intense peak of the measured spectrum.

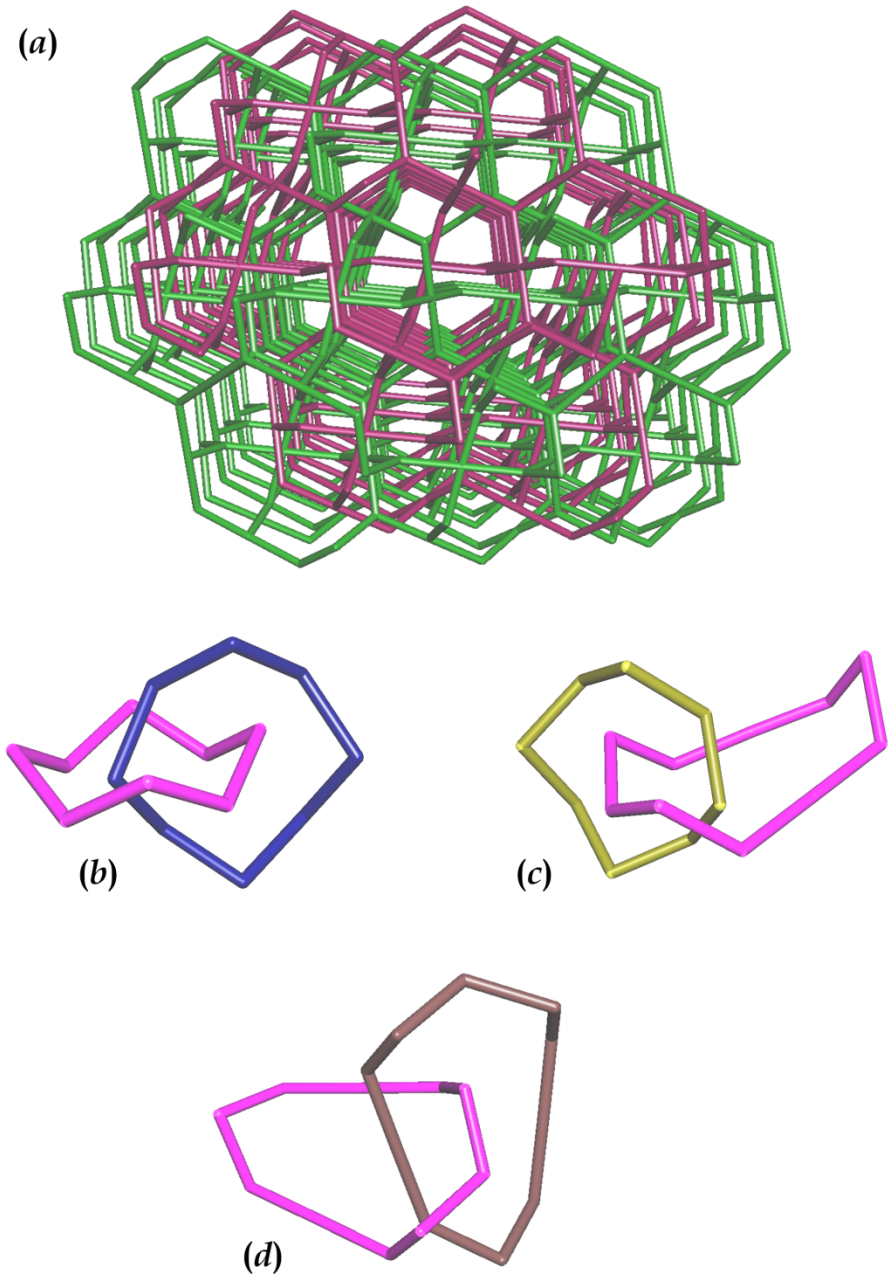

Figure S7. (a) Two interpenetrated nets of ***tbo***-type forming array of CuTATB, which show three different links (knots) of Hopf type between closed circles: (b) 8-membered (blue) and 8-membered (magenta); (c) 8-membered (yellow) and 10-membered (magenta); (d) 10-membered (brown) and 10-membered (magenta).

Topological analysis of CuTATB structure grown on the electrode surface has been performed using ToposPro software package [4]. All the interpenetration nets have the topology of ***tbo***-type net and the interpenetration type belongs to a class IIa [5]. As shown in Fig. S7, the interpenetration of two equivalent ***tbo***-nets realized by three kinds of interweaved rings (Hopf links): eight- and eight-membered rings (b); eight- and ten-membered rings (c); ten- and ten-membered rings (d).

4. SEM images of CuBTC grown on copper mesh

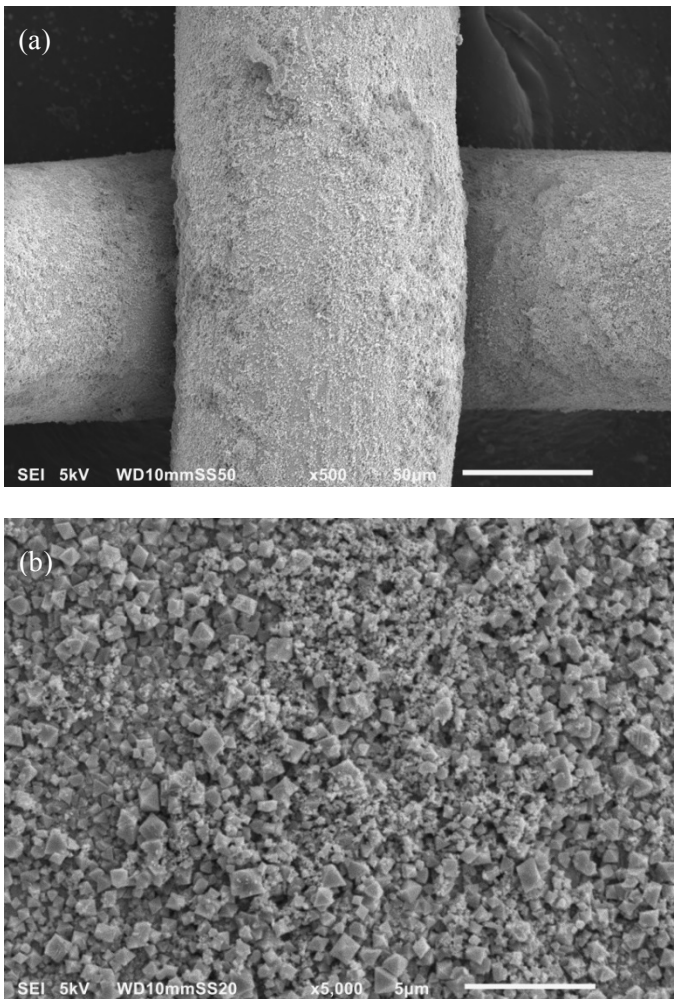

Figure S8. SEM micrographs of CuBTC grown on the surface of a copper mesh at different magnifications: ×500 (a) and ×5000 (b).

5. Sorption studies of electrochemically-grown MOFs

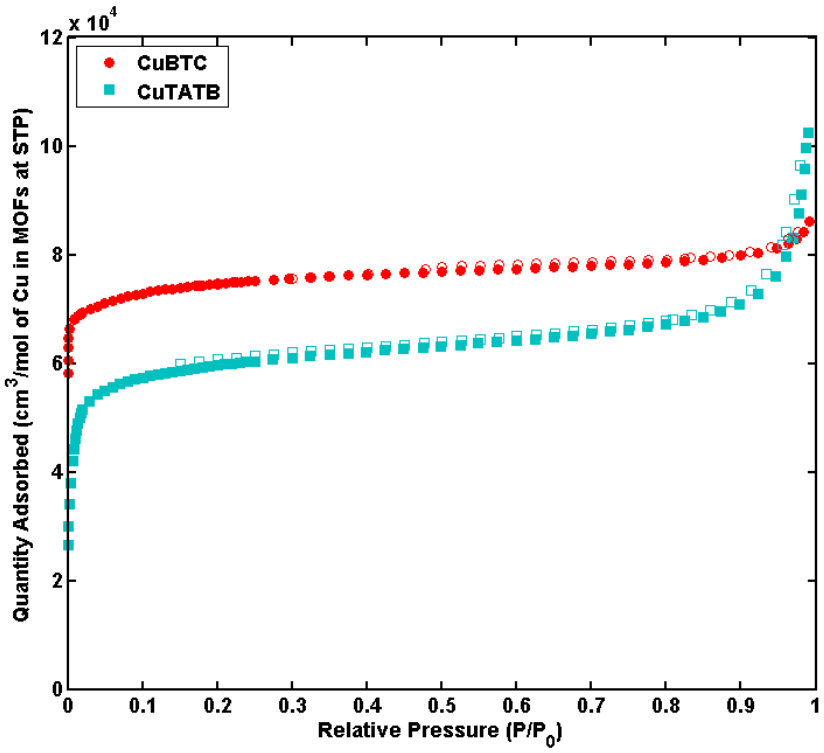

Figure S9. N_2 sorption isotherm (at 77 K) of CuBTC (red) and CuTATB (blue) synthesized as bulk powder.

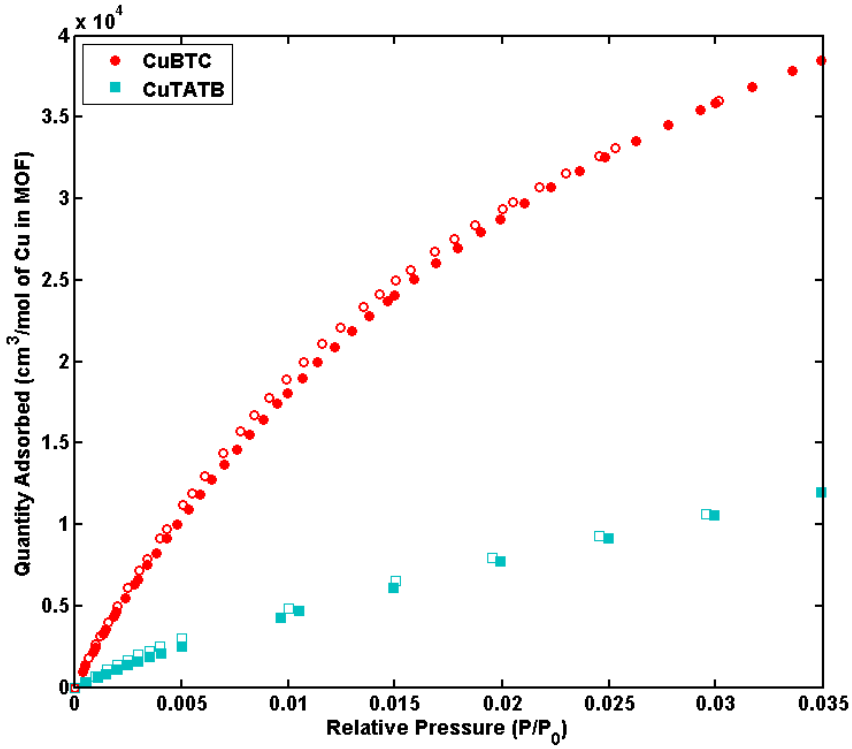

Figure S10. CO_2 sorption isotherm of bulk CuBTC (red) and CuTATB (blue) measured at 273K.

References

1. A. M. Joaristi, J. Juan-Alcaniz, P. Serra-Crespo, F. Kapteijn and J. Gascon, *Cryst Growth Des*, 2012, **12**, 3489-3498.
2. A. Altomare, C. Cuocci, C. Giacovazzo, A. Moliterni, R. Rizzi, N. Corriero and A. Falcicchio, *Journal of Applied Crystallography*, 2013, **46**, 1231-1235.
3. B. Mu, F. Li and K. S. Walton, *Chemical Communications*, 2009, 2493-2495.
4. V. A. Blatov, A. P. Shevchenko and D. M. Proserpio, *Cryst Growth Des*, 2014, **14**, 3576-3586.
5. I. A. Baburin, V. A. Blatov, L. Carlucci, G. Ciani and D. M. Proserpio, *Journal of Solid State Chemistry*, 2005, **178**, 2452-2474.